Brain Stimulation 12 (2019) 1402–1409

Contents lists available at ScienceDirect

Brain Stimulation

journal homepage: http://www.journals.elsevier.com/brain-stimulation

Theoretical principles of deep brain stimulation induced synaptic suppression

AmirAli Farokhniaee, Cameron C. McIntyre*

Department of Biomedical Engineering, Case Western Reserve University, Cleveland, OH, USA

ARTICLE INFO

Article history:
Received 25 February 2019
Received in revised form
6 July 2019
Accepted 8 July 2019
Available online 10 July 2019

Keywords:
Glutamate
Synapse
Thalamus
Basal ganglia
Cortex

ABSTRACT

Background: Deep brain stimulation (DBS) is a successful clinical therapy for a wide range of neurological disorders; however, the physiological mechanisms of DBS remain unresolved. While many different hypotheses currently exist, our analyses suggest that high frequency (~100 Hz) stimulation-induced synaptic suppression represents the most basic concept that can be directly reconciled with experimental recordings of spiking activity in neurons that are being driven by DBS inputs.
Objective: The goal of this project was to develop a simple model system to characterize the excitatory post-synaptic currents (EPSCs) and action potential signaling generated in a neuron that is strongly connected to pre-synaptic glutamatergic inputs that are being directly activated by DBS.
Methods: We used the Tsodyks-Markram (TM) phenomenological synapse model to represent depressing, facilitating, and pseudo-linear synapses driven by DBS over a wide range of stimulation frequencies. The EPSCs were then used as inputs to a leaky integrate-and-fire neuron model and we measured the DBS-triggered post-synaptic spiking activity.
Results: Synaptic suppression was a robust feature of high frequency stimulation, independent of the synapse type. As such, the TM equations were used to define alternative DBS pulsing strategies that maximized synaptic suppression with the minimum number of stimuli.
Conclusions: Synaptic suppression provides a biophysical explanation to the intermittent, but still time-locked, post-synaptic firing characteristics commonly seen in DBS experimental recordings. Therefore, network models attempting to analyze or predict the effects of DBS on neural activity patterns should integrate synaptic suppression into their simulations.

Introduction

The most common approach to modulate the nervous system with electrical stimulation is to use a brief stimulus pulse (~100 μs) to generate an extracellular electric field. This electric field can then manipulate the voltage sensor of sodium ion channels embedded in the membrane of neurons into generating a propagating action potential (AP). The basic point and purpose of generating the AP is to have it invade the synaptic terminals of the neuron and subsequently control the release of neurotransmitters with the explicit timing of the electrical stimuli [1]. However, the release of neurotransmitters from a synapse, as well as the resulting post-synaptic currents (PSCs), are dependent upon the firing history of the synapse [2]. Given that clinical stimulation technologies typically rely on a constant stimulation frequency, a key parameter of interest is the steady-state PSC generated at the synapse as a function of the stimulation frequency. In general, low stimulation frequencies (~10 Hz) can maintain high amplitude PSCs over prolonged periods of time; however, high stimulation frequencies (~100 Hz) typically suppress PSCs quickly after the onset of the stimulus train [3].

The concept of high frequency stimulation-induced suppression of synaptic transmission may be especially relevant to the therapeutic mechanisms of deep brain stimulation (DBS) [4]. The development of ~100 Hz DBS therapies have traditionally followed from the clinical foundation of ablative therapies performed within the same brain circuits [5]. In addition, the neurological disorders associated with successful DBS interventions are typically characterized by abnormal oscillatory activity within the afflicted brain networks [6]. As such, stimulation-induced suppression of synaptic communication in the directly activated neurons is consistent with

* Corresponding author. Department of Biomedical Engineering, Case Western Reserve University, 2103 Cornell Road, Rm 6224, Cleveland, OH, 44106, USA.
E-mail address: ccm4@case.edu (C.C. McIntyre).

https://doi.org/10.1016/j.brs.2019.07.005
1935-861X/

the general effect of ablation on neural activity, as well as the disruption of oscillatory signal transmission through a network.

Most in vivo experimental measures of DBS do not show a complete cessation of communication between the directly stimulated pre-synaptic neuron and a strongly connected post-synaptic neuron [e.g. Refs. [7,8]]. Instead, signal transmission that under low frequency stimulation is robust, becomes intermittent and low fidelity during high frequency stimulation, albeit still time-locked to the stimulus train. This suggests that DBS alters the dynamics of these synaptic connections, and ~100 Hz stimulation may act to filter the low frequency oscillatory activity of pre-synaptic neurons from influencing their post-synaptic neurons [9,10].

Detailed biophysical models of DBS have consistently shown robust AP initiation and propagation to ~100 Hz stimuli with ~100% fidelity in neurons that are in close proximity (~1 mm) to the stimulating electrode [e.g. Refs. [11,12]]. In addition, extensive axonal conduction parameter sensitivity studies suggest that DBS-induced APs are able to propagate to their axon terminals with a very high safety margin [e.g. Refs. [13,14]]. Therefore, while difficult to document experimentally, strong theoretical evidence supports the assumption of robust and high fidelity AP invasion of the synaptic terminals of directly stimulated neurons during DBS. Then if APs invade a synaptic bouton at high frequencies for long periods of time, the available experimental evidence clearly shows a marked suppression in the post-synaptic currents [15].

The general phenomenon of DBS-induced synaptic suppression can be most easily studied at glutamatergic synapses [16,17], where a wealth of experimental data exists to parameterize synaptic models, and synapticly generated APs time-locked to the stimuli can be monitored in post-synaptic neurons [18]. However, quantitative details on the specific effects of sustained high frequency synaptic driving are lacking in both the computational and experimental literature. In addition, multiple types of glutamatergic synapses are known to exist, including depressing, facilitating, and pseudo-linear [19]. Therefore, we set out to quantify how these different synapse types respond to DBS, and then used a leaky integrate-and-fire (LIF) neuron model to evaluate the post-synaptic effects on AP signaling. With this relatively simple model rooted in synaptic fundamentals, we then developed an analytical optimization of DBS pulsing to maximize synaptic suppression with the minimum number of stimuli.

Methods

The goal of this project was to develop a simple model system to characterize the excitatory post-synaptic currents (EPSCs) and action potential (AP) signaling generated in a neuron that is strongly connected to pre-synaptic glutamatergic inputs that are being directly activated by deep brain stimulation (DBS). We used the Tsodyks-Markram (TM) phenomenological synapse model to represent depressing (D), facilitating (F), and pseudo-linear (P) glutamatergic synapses driven by DBS over a wide range of stimulation frequencies. The post-synaptic EPSCs predicted by the DBS-driven TM synapses were then used as inputs to a leaky integrate-and-fire (LIF) neuron model that exhibited a stochastic background firing rate of ~20 Hz. The neuronal output of interest was the DBS-triggered post-synaptic spiking activity in the LIF neuron as a function of the DBS frequency.

Experimental example

The motivation for developing this DBS model system was to provide a simple biophysical explanation for the complex experimental peri-stimulus time histograms typically recorded from individual neurons that are being modulated by DBS-driven glutamatergic synaptic inputs [e.g. Refs. [7,8]]. Fig. 1 provides an example of the general concepts of interest, explicitly illustrating results from the work of Agensi et al. [8]. In those original experiments, DBS was applied in the thalamus (VPLo) and coupled with simultaneous single unit recordings in cortex (M1). They observed time-locked spiking activity in M1 neurons during DBS and plotted the stimulus-triggered APs as stacked raster plots over each inter-stimulus interval (~8 ms) for 1 min of 130 Hz thalamic DBS (7800 total pulses) (Fig. 1A). The example neuron shown in Fig. 1 was driven by a strong monosynaptic glutamatergic connection from directly activated neural elements in thalamus. However, during high frequency DBS, Agensi et al. [8] found that the entrainment patterns of cells in M1 never followed a one-to-one pattern of each stimulus pulse eliciting a unit-spike response in M1. Instead, the M1 neurons exhibited intermittent AP responses to the DBS-driven synaptic input, which tended to decrease in fidelity over time (Fig. 1A). These general DBS entrainment patterns are common for in vivo recordings of neurons that are being modulated by DBS-driven glutamatergic synaptic inputs [e.g. Refs. [16,17]]. Unfortunately, the biophysical mechanisms responsible for these experimental observations are only loosely defined [20], and computational models attempting to simulate neural network activity induced by DBS have historically ignored them. Therefore, we created a simple modeling infrastructure that can better account for the physiological realities of in vivo synaptic integration during DBS (Fig. 1B).

Synapse model

We used the Tsodyks-Markram (TM) [18,19] phenomenological model of short-term synaptic plasticity to quantify the dynamic behavior of glutamatergic synapses being driven by DBS-induced action potentials. TM models have the ability to simulate both short-term depression (associated with the depletion of neurotransmitter) and short-term facilitation (associated with the influx of calcium into the pre-synaptic terminal). The dynamics of the TM model arise from the combination of a depression effect, denoted by normalized variable x, which represents the fraction of neurotransmitter resources that remain available after synaptic transmission, and a facilitation effect modeled by utilization parameter u that represents the fraction of available neurotransmitter resources ready to be used (Fig. 2). As such, u is consumed to produce the postsynaptic current, I. The combination of the depression and facilitation effects, as well as the time delay, Δ, yields the following differential equations:

$$\dot{u} = -\frac{u}{\tau_f} + U(1-u^-)\delta(t-t_s-\Delta) \quad (1)$$

$$\dot{x} = -\frac{1-x}{\tau_d} - u^+x^-\delta(t-t_s-\Delta) \quad (2)$$

$$\dot{I} = -\frac{I}{\tau_s} + Au^+x^-\delta(t-t_s-\Delta) \quad (3)$$

where t_s is the spike time, δ is the Dirac delta function, U is the increment of u produced by an incoming spike, τ_f is the decay time constant of variable u, τ_d is the recovery time constant of variable x, τ_s is the decay time constant of variable I, and A denotes the synaptic response amplitude that would be produced with the release of all of the neurotransmitter resources (absolute synaptic response). The specific parameter values for the D, F, and P synapses are listed in Table 1, which were previously defined to match the experimentally measured characteristics of intracortical

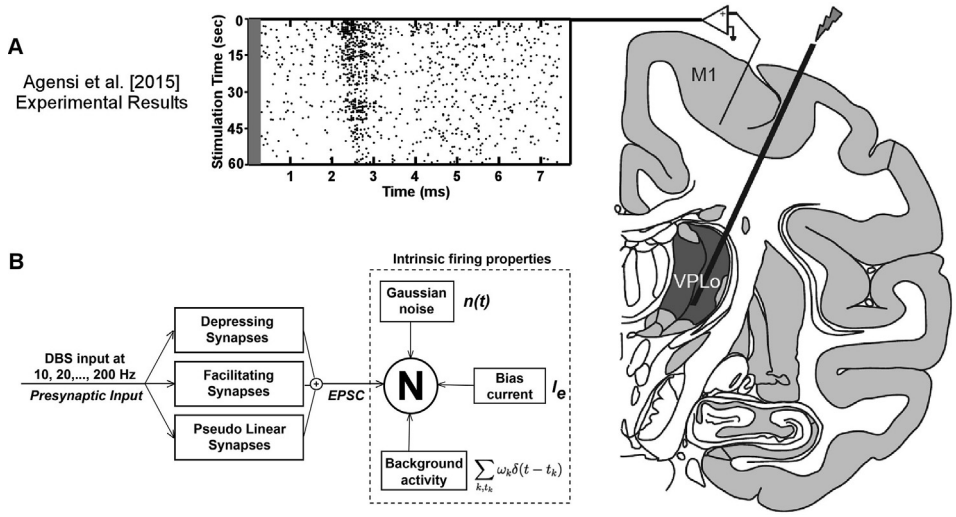

Fig. 1. Stimulus-triggered action potentials during DBS. A) Experimental results from Agensi et al. [8]. Raster plot of an M1 neuron during thalamic DBS. B) Model of DBS synaptic modulation of a neuron (N) with intrinsic firing.

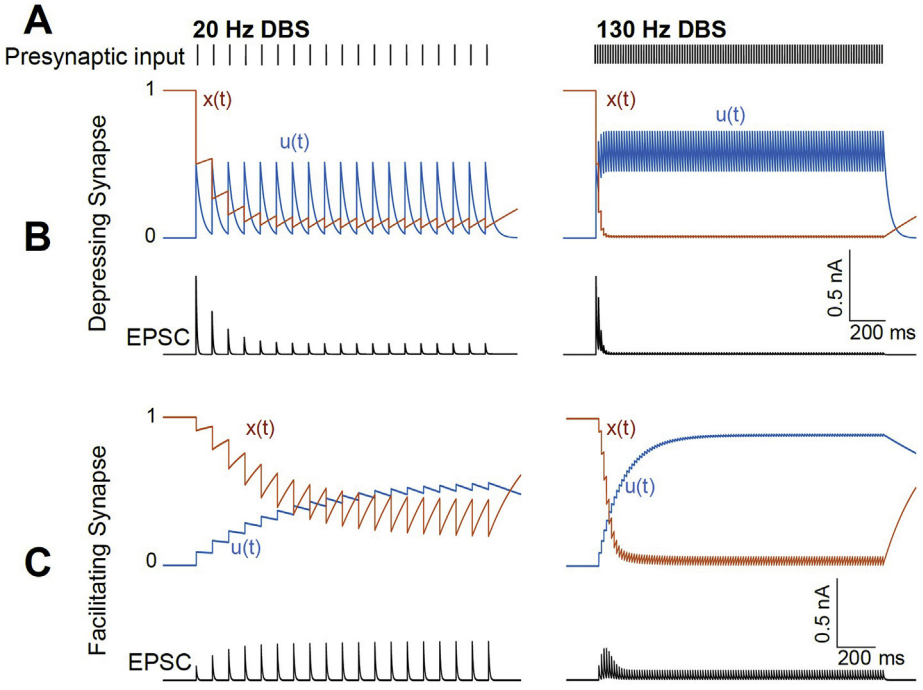

Fig. 2. TM synapse models. A) DBS pulses at 20 and 130 Hz for a duration of 1 s. B) Depressing synapse behavior. C) Facilitating synapse behavior.

Table 1

Synapse	τ_f (ms)	τ_d (ms)	τ_s (ms)	U	A (μA)
F	670	138	3	0.09	2.5
D	17	671	3	0.5	2.5
P	326	329	3	0.29	2.5

glutamatergic EPSCs [19]. The supplemental material also provides additional simulations where the synaptic parameters were varied to account for physiological ranges.

Post-synaptic neuron model

We used a noisy leaky-integrate-and-fire (LIF) neuron model [21,22] to evaluate the post-synaptic response to the DBS-driven synaptic inputs (Fig. 1B). The LIF neuron was parameterized to exhibit an intrinsic tonic firing pattern at ~20 Hz. This was achieved by incorporating a bias current, I_e (0.56 nA), background synaptic inputs that arrived stochastically at t_k via a Poissonian process with rate ω_k, and white Gaussian noise, $n(t)$, that had a mean of 0 and variance (σ^2) of 2.5. The LIF neuron also received glutamatergic inputs from DBS-driven synapses, where TM models simulated EPSCs that could also be modulated by a synaptic fidelity coefficient (ω_{sf}). Therefore, the transmembrane potential, v, of the LIF neuron model was defined by the following differential equation:

$$C_m\dot{v} = \frac{E_l - v}{R_m} + I_e + \omega_{sf}\, EPSC + \sum_{k,t_k}\omega_k\delta(t - t_k) + n(t) \quad (4)$$

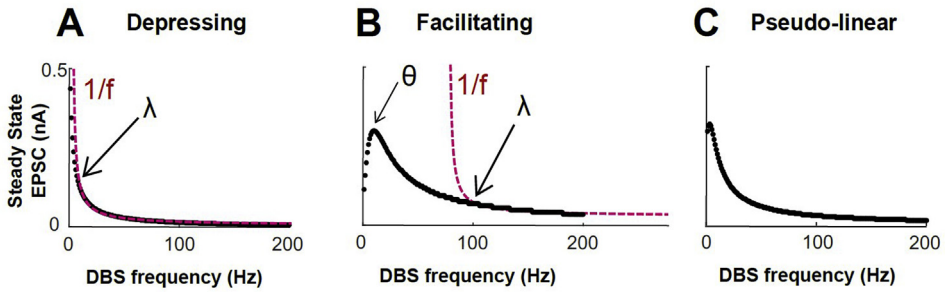

Fig. 3. Synaptic gain diagrams. Steady-state EPSC amplitude as a function of DBS frequency. A) Depressing synapse. B) Facilitating synapse. C) Pseudo-linear synapse. λ - limiting frequency, θ - peak frequency.

where C_m (1 μF) and R_m (100 MΩ) are the membrane capacitance and resistance respectively, and E_l (−70 mV) is the leak voltage. In eq. (4), and the results presented in Figs. 4–6, EPSC represents the summated post-synaptic currents from all DBS-driven inputs. The simulations were performed in MATLAB and the computer code for generating the results of this study is available on ModelDB (accession # to be defined at time of publication).

Results

Synaptic response to DBS

Simulations of the TM synaptic model demonstrate that low frequency stimulation can generate a wide range of EPSCs that depend upon the type of synapse (i.e. depressing (D), facilitating (F), or pseudo-linear (P)), as well as the timing of when the EPSC is being evaluated during the stimulus train (i.e. onset or steady-state) (Fig. 2). For a D synapse driven at 20 Hz, the number of available resources for transmission, *x*, decay with a fast time constant. This results in EPSCs that are initially very strong, but depress to a moderate amplitude in the steady-state (Fig. 2B). On the other hand, F synapses driven at 20 Hz exhibit an *x* that does not decay quickly because the usage fractions, *u*, are smaller. This results in EPSCs that are initially moderate in size, but increase over time to become higher amplitude in the steady-state (Fig. 2C). However, both the F and D synapses exhibit a similar trend of steady-state EPSC suppression under high frequency driving. F synapses depress to small EPSC amplitudes and D synapse EPSCs reduce to nearly zero during 130 Hz driving. Fig. 3 plots the steady-state amplitude of the post-synaptic currents as a function of the DBS frequency. Independent of the synapse type (D, F, P), high frequency driving of the synapse models generates marked EPSC suppression.

When an F synapse gets stimulated at progressively increasing DBS frequencies, the steady-state EPSC amplitude initially increases at lower frequencies and then decreases at higher frequencies, which produces a bell-shaped curve (Fig. 3B). The peak of the gain function is called the "peak frequency", which has a theoretical value given by Ref. [23]:

$$\theta = \frac{1}{\sqrt{U.\tau_f.\tau_d}} \tag{5}$$

For both F and D synapses, the gain diagrams decrease in 1/f

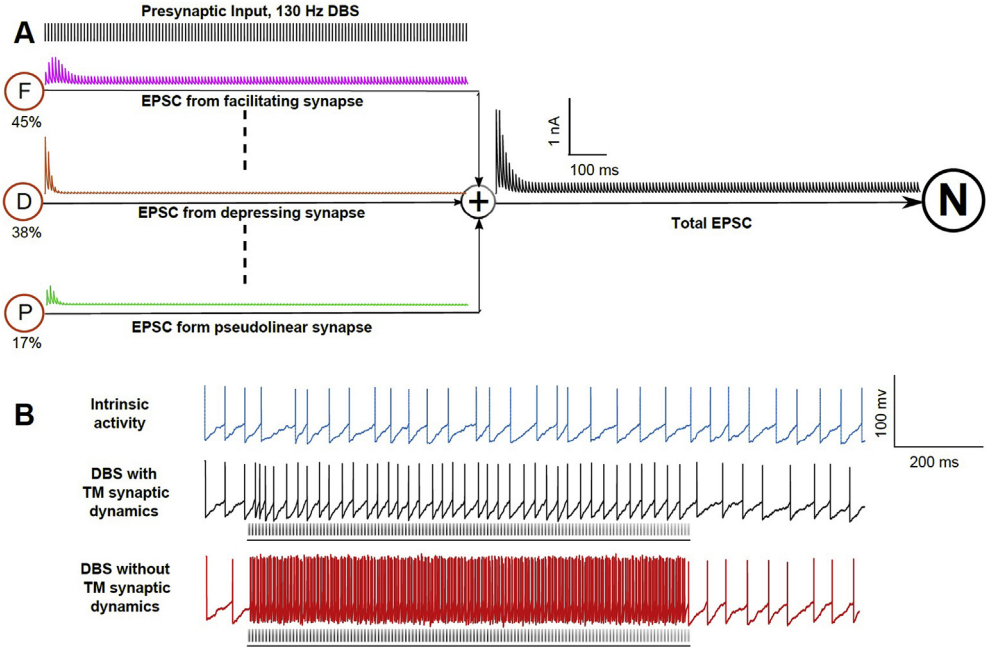

Fig. 4. DBS-driven synaptic modulation. A) 100 different synaptic inputs, driven by the DBS signal, to the LIF neuron model N. The distribution of F, D, and P synapse types is based on experimental estimates of their relative density in cortex. B) Response of N when driven by DBS inputs with or without TM synaptic dynamics.

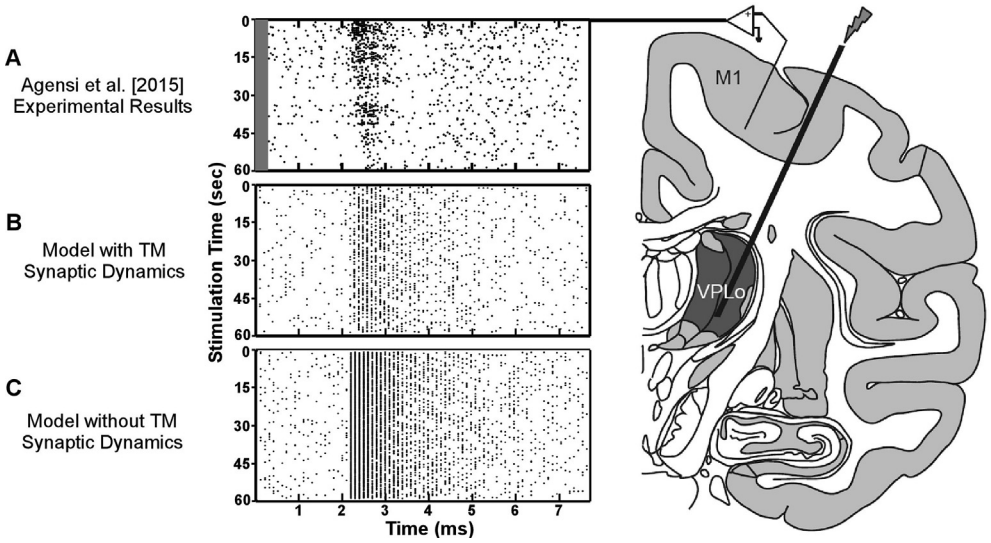

Fig. 5. Comparison with Agensi et al. [8] experimental results. A) Stimulus-triggered APs in M1 during thalamic DBS. B) Raster plot of the LIF model neuron model with TM synaptic dynamics. C) Raster plot of the LIF neuron model without TM synaptic dynamics.

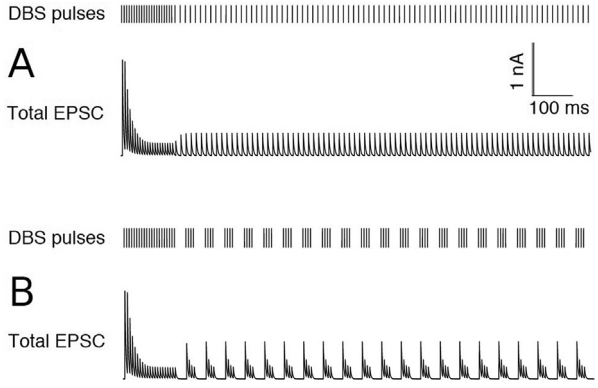

Fig. 6. Alternative DBS pulsing strategies. A) 130 Hz DBS pulses delivered at the onset of the stimulus train, followed by 95 Hz DBS pulses for tonic stimulation, maintains a suppressed total EPSC. B) 130 Hz DBS pulses delivered at the onset of the stimulus train, followed by 4 pulse DBS bursts delivered on a 50% duty cycle, maintains a suppressed total EPSC.

fashion, where f is the stimulation frequency. This characteristic is called the "limiting frequency", λ (Fig. 3A and B). Experimental measurements of λ range from 70 to 130 Hz for F synapses, and 5–30 Hz for D synapses [23]. Our specific TM synapse model parameterizations result in a λ of 11 Hz for the D synapse and 100 Hz for the F synapse [19]. Pseudo-linear synapses represent a combination of F and D behavior, but nonetheless also exhibits EPSC suppression at high stimulation frequencies.

Post-synaptic neuron firing

Given the EPSC modulation at individual synapses by DBS inputs (Fig. 3), the total EPSC for many synapses converging on an individual post-synaptic neuron will also be modulated. To simulate this phenomenon we created a LIF neuron model that received a total of 100 glutamatergic synaptic inputs, which were explicitly driven by our DBS signal (with a 2 ms AP transmission delay from thalamus). The various synaptic inputs were designated as F (45), D (38), or P (17) based on physiologically relevant distributions of the synapse types [19]. When a single DBS pulse was initiated in these synaptic inputs the EPSCs were generated simultaneously in the LIF neuron, thereby creating a total DBS EPSC that was a mix of F, D, and P components (Fig. 4A). A single DBS EPSC, generated with the initial conditions of the synapse models, was suprathreshold for the generation of a stimulus evoked AP in the LIF neuron. High frequency driving (130 Hz) of the DBS synaptic input generated an initial burst of APs in the LIF neuron and then as the total DBS EPSC reduced in amplitude to a steady-state value, the inputs provided subthreshold excitatory inputs to the LIF neuron (Fig. 4B). The overall result of this DBS-driven excitatory current was an increased average firing rate, but AP firing in the LIF neuron remained stochastic, albeit commonly time locked to a DBS input pulse.

The general firing characteristics achieved with TM synaptic dynamics are consistent with experimental recordings of post-synaptic glutamatergic modulation by DBS-driven inputs (Fig. 5) [e.g. Refs. [7,8]]. Alternatively, if we simply maintained the DBS EPSC at its initial conditions indefinitely, as done in nearly every DBS network model ever created, the response in the LIF neuron was a dramatic increase in firing that is not representative of typical experimental recordings (Figs. 4B and 5). Nonetheless, short-term synaptic suppression alone does not explain all of the features noted in the Agensi et al. [8] results. Other factors, such as spike timing dependent plasticity and recurrent inhibition, are likely responsible for the continued decay in synaptic fidelity over time and the reduced activity following the excitatory volley (see Discussion).

Analytical optimization of DBS pulsing

The majority of neurons with DBS-driven synaptic inputs are unlikely to be so strongly connected to those inputs that a single DBS-driven EPSC would be capable of generating an AP. As such, the primary effect of suppressing the steady-state EPSC on these more weakly connected neurons would be to even further minimize the post-synaptic influence from those DBS-driven connections. This follows the general hypothesis that a basic mechanism of high frequency DBS is the effective disconnection of directly stimulated neurons from their underlying brain networks via synaptic suppression [4,14,20].

Given the hypothesized goal of DBS-driven synaptic disconnection, we used the TM equations to design stimulation paradigms

that could similarly achieve the synaptic suppression observed with traditional tonic DBS, but with fewer stimuli. The key parameters for consideration are u (eq. (1)) and x (eq. (2)), where the basic concept is to minimize x and maximize u across the various synapse types that connect to the post-synaptic neuron (Fig. 2). Our goal was then to minimize the number of DBS pulses per unit time. One strategy to achieve that goal could be to use an initial burst of high frequency pulses to quickly push the system into the steady-state regime (Fig. 3), and then maintain the suppressed EPSCs by pulsing the system at a somewhat lower tonic frequency (Fig. 6A). The supplemental material provides an analytical optimization of this tonic stimulation concept using the TM equations. Fig. 6A demonstrates this DBS paradigm using 20 pulses at 130 Hz for the initial burst, followed by tonic stimuli every 10.5 ms (~95 Hz), using the overall model system as parameterized in Fig. 4.

A different optimization strategy would be to follow an initial burst of DBS pulses with subsequent bursts of DBS pulses delivered on a reduced duty cycle. Once again, the concept is to suppress the EPSCs at stimulation onset with a large burst, and then use smaller bursts to maintain the synaptic suppression (Fig. 6B). The supplemental material provides an analytical optimization of this burst stimulation concept using the TM equations. Fig. 6B demonstrates this DBS paradigm using 20 pulses at 130 Hz for the initial burst, followed by bursts with 4 pulses at 130 Hz delivered every 37 ms (~50% duty cycle), using the overall model system as parameterized in Fig. 4.

The quantitative details of truly optimizing these alternative stimulation paradigms for clinical effect would be dependent upon the specific axonal pathway(s) that are being directly modulated by DBS [24] and the specific synapse types associated with those connections [14]. As such, the examples in Fig. 6 simply provide a demonstration of the concept of synaptic suppression based DBS optimization. Nonetheless, these alternative DBS paradigms appear to show promise for reducing the total number of DBS pulses necessary to achieve a hypothesized neurophysiological mechanism of action.

Discussion

The goal of this study was to develop a simple model system that is capable of capturing the general features of DBS-induced synaptic suppression. We then used that model to demonstrate the relevance of synaptic suppression when analyzing experimental recordings of DBS peri-stimulus time histograms. Finally, we inverted the model to identify alternative DBS pulsing strategies that maximize the degree of synaptic suppression with the minimum number of stimuli. While the results of this study are only theoretical, they do represent a step toward dissecting the effects of DBS from the perspective of synaptic first principles. We propose that if we first understand the effects of DBS at the level of the synapse, we can then begin to extrapolate to analyses on network-level effects. However, ignoring the basics of DBS-induced synaptic dynamics while attempting to perform network activity analyses is unlikely to be a sound strategy.

We hypothesize that the fundamental goal of brain stimulation therapies is to use the electrical pulses to control the release of neurotransmitters in targeted brain circuits. Tenets of this hypothesis are that low frequency stimulation can be used to facilitate neurotransmitter release in directly activated pathways, while high frequency stimulation may suppress synaptic communication via the mechanisms described in this study. In vitro electrophysiology studies have long supported the general concepts of DBS-induced synaptic suppression [4,16,20]. In addition, recent computational studies [10,14] and intraoperative human recordings [17] have demonstrated the relevance of synaptic suppression in understanding and interpreting the neural activity patterns recorded during DBS. As such, we propose that explicit representation of DBS-induced synaptic dynamics is likely to be a key factor in developing physiologically accurate models of the network activity generated by DBS.

Computational models designed to study the network activity generated by DBS have historically ignored the role of synaptic plasticity in their analyses [e.g. Refs. [25–27]]. Instead, DBS network models have tended to focus on the interplay between static excitatory and inhibitory synaptic conductances in the generation of rhythmic bursting activity, and the subsequent disruption of that bursting activity with DBS. These models achieve burst disruption by overriding the underlying neural spiking and replacing it with high frequency activity that is permeated throughout the network. However, experimental recordings of DBS-induced neural activity do not coincide with these kinds of network model predictions (Figs. 1, 4 and 5).

Thankfully, not all DBS network models ignore synaptic plasticity. Rosenbaum et al. [10] applied the concepts of synaptic suppression to help explain in vivo experimental recordings of spiking activity in the basal ganglia during DBS. In addition, the Tass group has long focused on the role of spike timing dependent plasticity (STDP) in their attempts to develop stimulation patterns that induce therapeutic effects that persist after the cessation of stimulation [28,29]. They have used the physiological principles of STDP to more efficiently desynchronize network oscillations with novel stimulation strategies [30]. They call their stimulation method coordinated reset, and it has generated impressive therapeutic results in pre-clinical DBS experiments [31,32].

Synaptic plasticity consists of many different features that occur on different time scales [33,34]. Synaptic suppression is an acute effect that occurs on a short time scale (seconds). STDP is a longer lasting effect that occurs on the time scale of minutes. Then there are also intrinsic homeostatic control mechanisms regulating synaptic connections that act over a long time scale (hours). Our results show that synaptic suppression alone is insufficient to capture all of the features noted in the Agensi et al. [8] results (Fig. 5). We propose that STDP is likely to be responsible for the continued decay in synaptic fidelity over time in the experimental recordings. The TM equations do not account for STDP; however, wide-ranging mathematical algorithms are available to represent pair-based updates rules (i.e. the change in weight of a synapse depends on the temporal difference between pairs of pre- and post-synaptic spikes) [33]. It should also be noted that our analyses neglected the contribution of network dynamics in our simulations. As such, wide ranging network effects, such as increases or decreases in synchronization within the stimulated neural circuits, could also be playing an important role in the firing patterns recorded from the post-synaptic neurons. Therefore, a necessary step forward for the future of DBS network modeling is explicit integration of both short-term and long-term synaptic plasticity features into the simulations to evaluate the relative contribution of synapse-level effects vs. network-level effects in the DBS-induced activity patterns [10,35].

This study employed a simple phenomenological model of short-term synaptic dynamics [18], albeit explicitly parameterized to match glutamateric synapses in the rodent cortex [19]. Given the recent focus on direct cortical modulation from DBS in therapeutic mechanisms research [e.g. Refs. [36,37]], we considered the available cortical synapse models highly relevant to DBS. However, one caveat is that human synapses appear to have faster dynamics than the rodent [38]. Nonetheless, an important conclusion from our analyses is that the specific details of the synapse model (e.g. F or D) are somewhat irrelevant under the conditions of high frequency driving (Fig. 3), as they all exhibit suppression. As such, the general

findings we noted for cortical synaptic connections may also be applicable to synapses in the basal ganglia [10]. Further, the structure of both the excitatory and inhibitory versions TM equations is the same [19]. Therefore, synaptic suppression may also be occurring at DBS-driven GABAergic IPSCs, as suggested by recent experimental studies [39,40].

One important limitation of the TM synapse model is the failure to explicitly account for multiple pools of synaptic vesicles [41]. Detailed analyses of synaptic vesicles suggest there is a readily releasable pool, readily priming pool, premature pool, and resting pool [42]. Under high frequency stimulation conditions, the depletion and replenishment of these various pools can be difficult to estimate [15], and high frequency stimulation has been shown to enhance the rate of replenishment [43,44]. Unfortunately, the details of replenishment during long-term high frequency stimulation are currently undocumented. This gap in knowledge represents an important opportunity for collaboration between the basic science of synaptic physiology and the clinical application of DBS technology.

DBS research is currently benefiting from large funding initiatives, sponsored by both government and industry, which focus on understanding the brain network connections and neural activity patterns that underlie disease states, as well as their modulation by stimulation. A contribution of this study to that larger body of work is an alternative perspective that many of the network-level responses generated by DBS may be rooted in the biophysics of the individual synapses that are being driven by DBS. We propose that exploiting the physiological limits of the synaptic machinery to effectively suppress connectivity is a basic mechanism of DBS, and a simple model of those processes can be used to help guide optimization of DBS pulsing.

Conflicts of interest

CCM is a paid consultant for Boston Scientific Neuromodulation, receives royalties from Hologram Consultants, Neuros Medical and Qr8 Health, and is a shareholder in the following companies: Hologram Consultants, Surgical Information Sciences, Cortics, Autonomic Technologies, Cardionomic, Enspire DBS.

Acknowledgement

This work was supported by the National Institutes of Health (R01 NS086100).

Appendix A. Supplementary data

Supplementary data to this article can be found online at https://doi.org/10.1016/j.brs.2019.07.005.

References

[1] McIntyre CC, Anderson RW. Deep brain stimulation mechanisms: the control of network activity via neurochemistry modulation. J Neurochem 2016;139(Suppl1):338–45.
[2] Zucker RS, Regehr WG. Short-term synaptic plasticity. Annu Rev Physiol 2002;64:355–405.
[3] Neher E, Sakaba T. Multiple roles of calcium ions in the regulation of neurotransmitter release. Neuron 2008;59(6):861–72.
[4] Urbano FJ, Leznik E, Llinas RR. Cortical activation patterns evoked by afferent axons stimuli at different frequencies: an in vitro voltage-sensitive dye imaging study. Thalamus Relat Syst 2002;1:371–8.
[5] Lozano AM, Lipsman N. Probing and regulating dysfunctional circuits using deep brain stimulation. Neuron 2013;77(3):406–24.
[6] McIntyre CC, Hahn PJ. Network perspectives on the mechanisms of deep brain stimulation. Neurobiol Dis 2010;38(3):329–37.
[7] Hashimoto T, Elder CM, Okun MS, Patrick SK, Vitek JL. Stimulation of the subthalamic nucleus changes the firing pattern of pallidal neurons. J Neurosci 2003;23(5):1916–23.
[8] Agnesi F, Muralidharan A, Baker KB, Vitek JL, Johnson MD. Fidelity of frequency and phase entrainment of circuit-level spike activity during DBS. J Neurophysiol 2014;114(2):825–34.
[9] Rosenbaum R, Rubin J, Doiron B. Short term synaptic depression imposes a frequency dependent filter on synaptic information transfer. PLoS Comput Biol 2012;8(6):e1002557.
[10] Rosenbaum R, Zimnik A, Zheng F, Turner RS, Alzheimer C, Doiron B, Rubin JE. Axonal and synaptic failure suppress the transfer of firing rate oscillations, synchrony and information during high frequency deep brain stimulation. Neurobiol Dis 2014;62:86–99.
[11] McIntyre CC, Grill WM, Sherman DL, Thakor NV. Cellular effects of deep brain stimulation: model-based analysis of activation and inhibition. J Neurophysiol 2004;91(4):1457–69.
[12] Miocinovic S, Parent M, Butson CR, Hahn PJ, Russo GS, Vitek JL, McIntyre CC. Computational analysis of subthalamic nucleus and lenticular fasciculus activation during therapeutic deep brain stimulation. J Neurophysiol 2006;96:1569–80.
[13] Grill WM, Cantrell MB, Robertson MS. Antidromic propagation of action potentials in branched axons: implications for the mechanisms of action of deep brain stimulation. J Comput Neurosci 2008;24(1):81–93.
[14] Anderson RW, Farokhniaee A, Gunalan K, Howell B, McIntyre CC. Action potential initiation, propagation, and cortical invasion in the hyperdirect pathway during subthalamic deep brain stimulation. Brain Stimul 2018;11(5):1140–50.
[15] Thanawala MS, Regehr WG. Determining synaptic parameters using high-frequency activation. J Neurosci Methods 2016;264:136–52.
[16] Anderson TR, Hu B, Iremonger K, Kiss ZH. Selective attenuation of afferent synaptic transmission as a mechanism of thalamic deep brain stimulation-induced tremor arrest. J Neurosci 2006;26(3):841–50.
[17] Milosevic L, Kalia SK, Hodaie M, Lozano AM, Popovic MR, Hutchison WD. Physiological mechanisms of thalamic ventral intermediate nucleus stimulation for tremor suppression. Brain 2018;141(7):2142–55.
[18] Tsodyks MV, Markram H. The neural code between neocortical pyramidal neurons depends on neurotransmitter release probability. Proc Natl Acad Sci U S A 1997;94(2):719–23.
[19] Markram H, Muller E, Ramaswamy S, Reimann MW, Abdellah M, Sanchez CA, Ailamaki A, Alonso-Nanclares L, Antille N, Arsever S, Kahou GA, Berger TK, Bilgili A, Buncic N, Chalimourda A, Chindemi G, Courcol JD, Delalondre F, Delattre V, Druckmann S, Dumusc R, Dynes J, Eilemann S, Gal E, Gevaert ME, Ghobril JP, Gidon A, Graham JW, Gupta A, Haenel V, Hay E, Heinis T, Hernando JB, Hines M, Kanari L, Keller D, Kenyon J, Khazen G, Kim Y, King JG, Kisvarday Z, Kumbhar P, Lasserre S, Le Bé JV, Magalhães BR, Merchán-Pérez A, Meystre J, Morrice BR, Muller J, Muñoz-Céspedes A, Muralidhar S, Muthurasa K, Nachbaur D, Newton TH, Nolte M, Ovcharenko A, Palacios J, Pastor L, Perin R, Ranjan R, Riachi I, Rodríguez JR, Riquelme JL, Rössert C, Sfyrakis K, Shi Y, Shillcock JC, Silberberg G, Silva R, Tauheed F, Telefont M, Toledo-Rodriguez M, Tränkler T, Van Geit W, Díaz JV, Walker R, Wang Y, Zaninetta SM, DeFelipe J, Hill SL, Segev I, Schürmann F. Reconstruction and simulation of neocortical microcircuitry. Cell 2015;163(2):456–92.
[20] Iremonger KJ, Anderson TR, Hu B, Kiss ZH. Cellular mechanisms preventing sustained activation of cortex during subcortical high-frequency stimulation. J Neurophysiol 2006;96(2):613–21.
[21] Stein RB. A theoretical analysis of neuronal variability. Biophys J 1965;5:173–94.
[22] Abbot LF, Kepler TB. In: Danto L, editor. Statistical mechanics of neural networks. Berlin: Springer; 1990.
[23] Markram H, Wang Y, Tsodyks M. Differential signaling via the same axon of neocortical pyramidal neurons. Proc Natl Acad Sci U S A 1998;95(9):5323–8.
[24] Gunalan K, Howell B, McIntyre CC. Quantifying axonal responses in patient-specific models of subthalamic deep brain stimulation. Neuroimage 2018;172:263–77.
[25] Rubin JE, Terman D. High frequency stimulation of the subthalamic nucleus eliminates pathological thalamic rhythmicity in a computational model. J Comput Neurosci 2004;16(3):211–35.
[26] Hahn PJ, McIntyre CC. Modeling shifts in the rate and pattern of subthalamopallidal network activity during deep brain stimulation. J Comput Neurosci 2010;28(3):425–41.
[27] Kumaravelu K, Brocker DT, Grill WM. A biophysical model of the cortex-basal ganglia-thalamus network in the 6-OHDA lesioned rat model of Parkinson's disease. J Comput Neurosci 2016;40(2):207–29.
[28] Tass PA. A model of desynchronizing deep brain stimulation with a demand-controlled coordinated reset of neural subpopulations. Biol Cybern 2003;89(2):81–8.
[29] Hauptmann C, Popovych O, Tass PA. Effectively desynchronizing deep brain stimulation based on a coordinated delayed feedback stimulation via several sites: a computational study. Biol Cybern 2005;93(6):463–70.
[30] Popovych OV, Tass PA. Desynchronizing electrical and sensory coordinated reset neuromodulation. Front Hum Neurosci 2012;6:58.
[31] Tass PA, Qin L, Hauptmann C, Dovero S, Bezard E, Boraud T, Meissner WG. Coordinated reset has sustained aftereffects in Parkinsonian monkeys. Ann Neurol 2012;72(5):816–20.
[32] Wang J, Nebeck S, Muralidharan A, Johnson MD, Vitek JL, Baker KB. Coordinated reset deep brain stimulation of subthalamic nucleus produces long-lasting, dose-dependent motor improvements in the 1-Methyl-4-phenyl-

1,2,3,6-tetrahydropyridine non-human primate model of parkinsonism. Brain Stimul 2016;9(4):609–17.
[33] Morrison A, Diesmann M, Gerstner W. Phenomenological models of synaptic plasticity based on spike timing. Biol Cybern 2008;98(6):459–78.
[34] Turrigiano GG. The self-tuning neuron: synaptic scaling of excitatory synapses. Cell 2008;135(3):422–35.
[35] Manos T, Zeitler M, Tass PA. How stimulation frequency and intensity impact on the long-lasting effects of coordinated reset stimulation. PLoS Comput Biol 2018;14(5):e1006113.
[36] Sanders TH, Jaeger D. Optogenetic stimulation of cortico-subthalamic projections is sufficient to ameliorate bradykinesia in 6-ohda lesioned mice. Neurobiol Dis 2016;95:225–37.
[37] Miocinovic S, de Hemptinne C, Chen W, Isbaine F, Willie JT, Ostrem JL, Starr PA. Cortical potentials evoked by subthalamic stimulation demonstrate a short latency hyperdirect pathway in humans. J Neurosci 2018;38(43):9129–41.
[38] Testa-Silva G, Verhoog MB, Linaro D, de Kock CP, Baayen JC, Meredith RM, De Zeeuw CI, Giugliano M, Mansvelder HD. High bandwidth synaptic communication and frequency tracking in human neocortex. PLoS Biol 2014;12(11):e1002007.
[39] Liu LD, Prescott IA, Dostrovsky JO, Hodaie M, Lozano AM, Hutchison WD. Frequency-dependent effects of electrical stimulation in the globus pallidus of dystonia patients. J Neurophysiol 2012;108(1):5–17.
[40] Milosevic L, Kalia SK, Hodaie M, Lozano AM, Fasano A, Popovic MR, Hutchison WD. Neuronal inhibition and synaptic plasticity of basal ganglia neurons in Parkinson's disease. Brain 2018;141(1):177–90.
[41] Neher E. Merits and limitations of vesicle pool models in view of heterogeneous populations of synaptic vesicles. Neuron 2015;87(6):1131–42.
[42] Qiu X, Zhu Q, Sun J. Quantitative analysis of vesicle recycling at the calyx of Held synapse. Proc Natl Acad Sci U S A 2015;112(15):4779–84.
[43] Wang LY, Kaczmarek LK. High-frequency firing helps replenish the readily releasable pool of synaptic vesicles. Nature 1998;394(6691):384–8.
[44] Sakaba T. Roles of the fast-releasing and the slowly releasing vesicles in synaptic transmission at the calyx of Held. J Neurosci 2006;26(22):5863–71.